

## ULTRASONIC IMAGING IN MERCURY

R A Bacon (1), C J K McIntee (2), N MacCuaig (3)

- (1) University of Surrey, Department of Physics, Guildford, Surrey.
- (2) British Steel Technical, Teesside Labs. Middlesbrough, Cleveland.
- (3) Surrey Medical Imaging Systems, Ltd., Surrey Research Park, Guildford.

### ABSTRACT

Gross surface deformations in liquid mercury have been imaged using ultrasonic computer assisted tomography. The deformations have been caused by jets of gas impinging on the liquid surface. Information about the geometry of the cavities formed by the jets has been obtained from reconstructions of the mercury gas interface in planes parallel to the surface at varying depths. Early results indicate that information may also be available about short term instabilities in the shape of the cavities.

### 1. INTRODUCTION

The work described here has been carried out as a result of continuing interest in the mechanisms of top blown steelmaking. Top blown steelmaking takes several forms, but in essence jets of oxygen produced by a cluster of one or more De Laval nozzles operated under supersonic conditions impinge on the surface of the liquid iron. Deep cavities are produced in the liquid accompanied by oscillation of the liquid surface and the shearing of large quantities of droplets from the surface. Oxygen from the gas jets reacts with carbon and silicon in the impure iron to produce steel. The shape and size of the cavities affects both the bulk stirring of liquid iron and the local refining rate. Optimum operation of the process depends on a careful balance between local oxidation and the transport of fresh iron to the gas/liquid interface. Cavity dimensions and stability depend critically upon the ambient pressure above the bath surface, the number and geometry of the nozzles and the driving pressure of the oxygen on the upstream side of the nozzles.

In order to investigate some of these process parameters, a laboratory model was constructed using mercury as the model fluid representing liquid steel. The model consists of a ladle containing up to 1000kg of mercury standing in the base of a gas tight steel pressure vessel 1.2m high and 0.5m diameter. The pressure vessel is connected to a pumping system to allow ambient pressure control and extraction of toxic vapour. Viewing windows are arranged just above the mercury level to allow observation of the mercury surface while nitrogen gas is being jetted onto it. The gas supply tube which holds the nozzle cluster is positioned 160mm above the surface.

### 2. COMPUTER ASSISTED TOMOGRAPHY.

The reconstruction algorithm used, filtered back-projection, is the same as that frequently used in X-ray or other tomographic scanning [1]. It is assumed that there is a real two dimensional distribution of some property, given by  $f(x,y)$  or  $f(r,\vartheta)$ , and it is further assumed that this function has a value of zero outside a circle of some diameter. In X-ray tomography this function would be taken as representing the attenuation of the radiation in the medium. The distribution of the function in the medium is interrogated by means of many beams of the radiation, each beam providing a value representing the total attenuation along its path. i.e.

$$p(r,\vartheta) = \int_s f(r,\vartheta) ds$$

where the line  $s$  is defined by  $r = x \cos\vartheta + y \sin\vartheta$  as shown in figure 1.  $p(r,\vartheta)$  is known as a *line integral*.

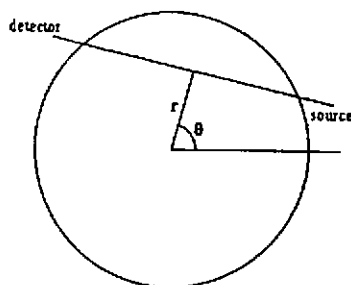


Figure 1. - Geometry of a line integral.

The information obtained from measurements consists of sets of line integrals  $p(r,\vartheta)$  ( $-\ell \leq r \leq \ell$ ) for a range of values of  $\vartheta$ , ( $0 \leq \vartheta \leq \pi$ ). In order to reconstruct an approximation  $b(r,\vartheta)$  to the original distribution  $f(r,\vartheta)$ , the ray sums may be 'back-projected' across an image area, so that

$$b(r,\vartheta) = \int_0^\pi p(r \cos(\vartheta - \varphi), \varphi) d\varphi$$

This can be visualised for a given  $r$  and  $\vartheta$  as a sum of line integrals, one from each set, chosen so that each line passes through the point  $(r,\vartheta)$ . The integration is over  $\varphi$  from 0 to  $\pi$ , since the original line integrals were obtained over this range. This is illustrated in figure 2.

The direct application of this algorithm leads to a significant over-estimation of the function  $f(r,\vartheta)$  at each pixel (picture element). This can be appreciated quite simply by observing that the line integrals will all be positive valued, so that the subsequent 'back projection' contributes only

## IMAGING IN MERCURY

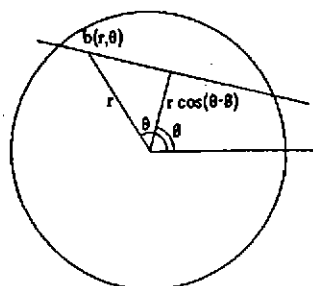


Figure 2. - Back projection geometry

positive values to the function estimation. A filter function can be applied to the sets of line integrals before they are 'back-projected' in order to correct for this effect. The effect of this filtering is illustrated in figure 3, which shows the reconstruction of a small rectangular test object with an L shaped cavity.

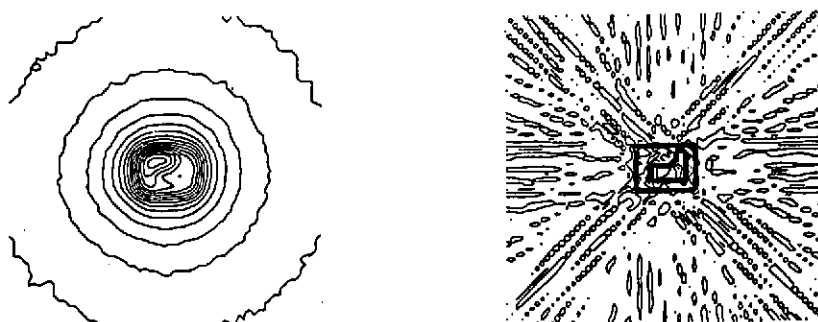


Figure 3. Left - Unfiltered back-projection.  
Right - Filtered back-projection.

The use of transmission ultrasonics in a tomographic modality is not new [2]. Measurements commonly used for reconstructions are the ultrasonic attenuation and velocity, both in soft tissue [3] and in other materials [4].

### 3. THE EXPERIMENTAL ARRANGEMENT

The purpose of the ultrasonic scanning was to obtain the positions of the mercury/air interfaces of the depressions caused by three gas jets emanating from the lance. These depressions were typically a few tens of millimetres deep, the exact depth depending upon factors such as the lance height above

# Proceedings of the Institute of Acoustics

## IMAGING IN MERCURY

the liquid surface, the gas pressure, the ambient pressure and the dimensions and form of the gas jet orifices.

In order to produce the data necessary for a tomographic reconstruction of the surfaces in a plane within the mercury, it was necessary to obtain a measure of the amplitude of an ultrasonic beam when it had traversed the sample area. This had to be repeated at a number of positions across the sample area, and then the orientation of the beam changed and the sequence repeated. Thus, the transducers would normally be required to translate across the sample area and also to rotate around it. In practice, since even this room temperature environment was relatively inhospitable (with much splashing of mercury), the translation motor was sited outside the chamber and the movement transmitted into the pressure chamber through a gland fitting. Then, instead of the transducer mounting rotating around the vessel, the lance and thus the gas jets were rotated. Since the vessel was circular and the depressions being investigated were functions of the lance orifices, the two rotations were considered equivalent.

In order to be able to appraise the surfaces of the depressions, it was necessary to reconstruct the boundaries at different depths. Rather than effect another plane of movement of the transducers, a mounting was devised that allowed four pairs of transducers to be set up at four different depths. This removed the requirement for more than one gland fitting through the chamber wall, and meant that scans at more than one depth could be made at the same time. The arrangement of the transducer mounting and scanning mechanism is illustrated in figure 4.

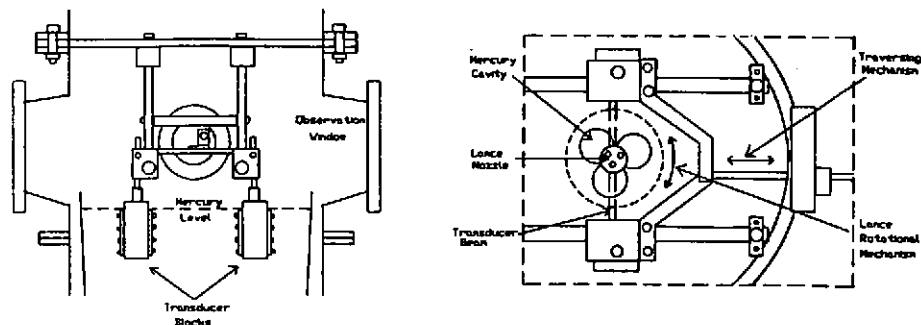


Figure 4.

Left - scanning mechanism (end view) in pressure vessel.

Right - Scanning mechanism (top view) in relation to cavities.

As far as the acoustic problems were concerned, mercury and water share about the same acoustic velocity but, of course, mercury has a significantly higher density. In fact this merely improves the coupling between the transducers and the liquid, since the acoustic impedance of mercury is nearer that of the transducer material. The transducers used were plane with elements 10mm in

## IMAGING IN MERCURY

diameter mounted in 16mm diameter housings. The transducer mountings were designed to be suitable for water immersion, but gave some trouble when used in mercury. Most transducers would work correctly for a short while, and then malfunction. Upon removal from the mercury they would be found to operate correctly in water, for example, only to malfunction again when put back into mercury. Four transducers were found to operate reliably in mercury.

A block diagram of the experimental arrangement is given in figure 5. The controlling computer, a PC/AT compatible controlled the stepping motors and the data acquisition via an IEEE488 interface. A Baugh and Weedon model PA1020 flaw detector was used to generate the interrogative pulse and amplify it for the transmitter at a pulse repetition rate of about 1000 Hz. The output from the receiver was detected, rectified and gated by the same unit, thus providing an analogue signal proportional to the amplitude of the received ultrasonic signal. The magnitude of this signal was time averaged and digitised for each position of the transducers. Thus for each beam position and orientation a number was obtained that was proportional to the received ultrasonic signal strength.

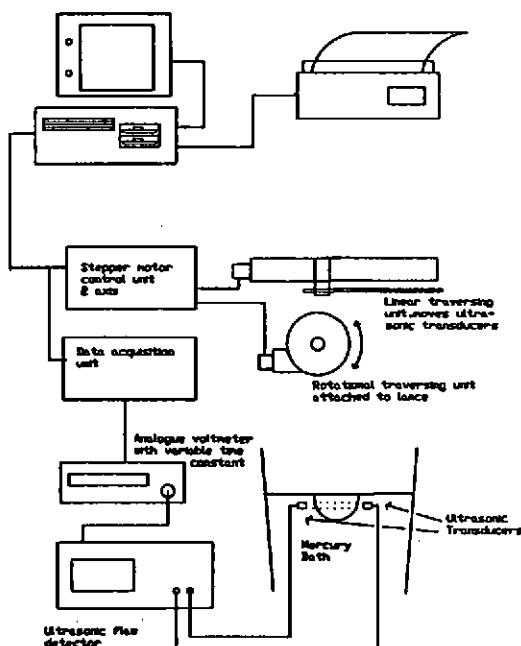


Figure 5 - the experimental system.

## 4. RESULTS AND DISCUSSION

The values obtained as described above were originally taken to represent the degree to which the beam of ultrasound was not obscured by the surface depressions. The depressions caused by the gas jets were very dynamic, and the surfaces could be observed (through the spray of mercury) to be of very rough texture. Thus it was assumed that if any part of a beam was incident upon such a surface then that component of the beam would be scattered through large angles, even if originally at grazing incidence.

Contour plots of this supposed 'signal obscuration' at two different depths

## IMAGING IN MERCURY

are shown in figure 6. Here three cavities are clearly visible, with a well defined circular gradient in the mapped parameter at each site. The gradient of this parameter is greater and the range of values is also greater in measurements made at the shallower depth. The beam width is of the order of 10mm, but the regions of approximately constant gradients extend over about 20mm, thus making it unlikely that they are the result of the progressive obscuration of the beam.

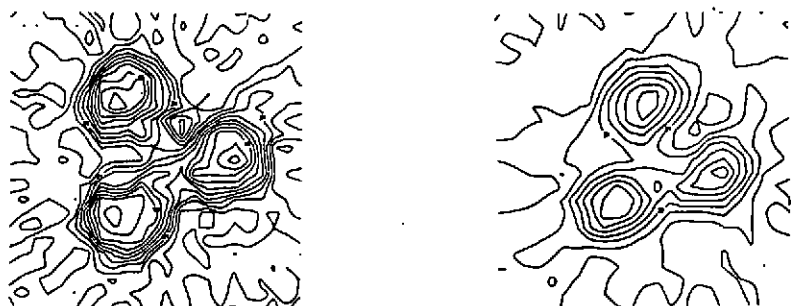


Figure 6 - contour maps obtained at (left) 12mm depth and (right) 16mm depth. The sample area is approximately 160mm by 160mm.

In order to investigate the nature of the interaction between the ultrasound and the liquid/gas surfaces, a computer based electronic phantom was developed that could generate line integrals according to a variety of modelled physical criteria. A simple model test object having three approximately circular objects was defined, and line integrals were generated according to three types of interaction. In each of these the liquid was assumed to have no effect upon the signal. The first interaction type was based upon the concept of an attenuating medium, and merely introduced an attenuation proportional to the depth of object material traversed by each line. The second modelled the assumed interaction, and the amplitude was reduced according to the overlap of each beam path with any of the three objects. The third anticipated some planned time-dependant analysis of the cavities, and assumed the overlap model of the previous interaction but coupled to a probability that the cavity surface would actually be at the point in question at the time of the measurement. As far as the real measurements are concerned, the long time averaging of the received signal amplitude generates a value proportional to this probability. The contours reconstructed from the data produced by these three models are shown in figures 7, 8 and 9. The first model produces the well defined objects that would be expected, with very sharp gradients at their edges. The second produces little more than a circle round the outside edges of the three objects, with a little internal structure. The third, based upon a dynamic model of the shapes of the cavities, displays similar gradients to those obtained experimentally.

## IMAGING IN MERCURY

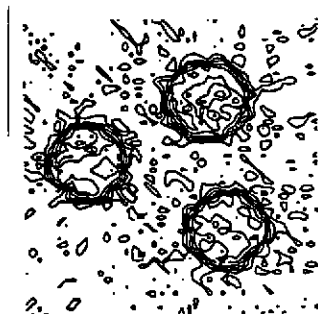


Figure 7 - contour plot of reconstruction of attenuating model.

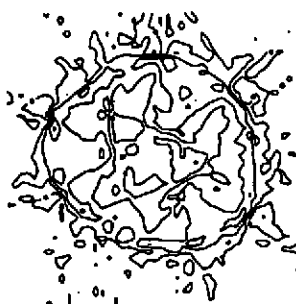


Figure 8 - simple beam model

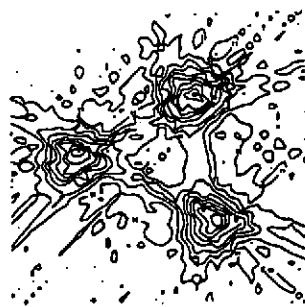


Figure 9 - dynamic cavity model

### 5. CONCLUSIONS

Ultrasonic tomographic methods have been applied to an unusual situation, with initially optimistic results. The nature of the ultrasonic to liquid/gas interface requires more investigation before the property that is being imaged can be stated with confidence. It would appear from some simple computer modelling that the images give information about the change in shape and size of the cavities as well as about their position.

### 6. REFERENCES

1. R A Brooks and G DiChiro. 'Principles of Computer Assisted Tomography (CAT) in Radiographic and Radioisotope Imaging'. J.C.A.T., 2, 1978.

# Proceedings of the Institute of Acoustics

## IMAGING IN MERCURY

2. Wade G, Mueller R K, and Kayeh M, 'A Survey of Techniques for Ultrasonic Tomography'. Pages 165-215 in 'Computer Aided Tomography and Ultrasonics in Medicine'. Raviv et al. (eds.) North Holland, 1979.
3. Greenleaf J F and Bahn R C, 'Clinical Imaging with Transmissive Ultrasonic Computerized Tomography', IEEE Trans. Bio. Eng. 2, 177-186, 1981.
4. Hildebrand B P and Harrington T P, 'Mapping of Materials Stress with Ultrasonic Tomography'. Mater. Eval. (USA) 39, 383-390, 1981.